MEASUREMENT AND DYNAMIC DISPLAY OF ACOUSTIC WAVE PULSES*

J-y. Lu, T. Kinter, and J. F. Greenleaf

Biodynamics Research Unit, Department of Physiology and Biopyysics,
Mayo Clinic/Foundation, Rochester, MN 55905

ABSTRACT

To evaluate and improve the longitudinal and lateral resolution of an ultrasonic transducer in pulse-echo imaging, it is useful to visualize how the ultrasonic pulse travels in space. This paper develops a method for measuring and dynamically displaying the traveling acoustic wave pulses. A half millimeter hydrophone was used to scan two-dimensional planes through the beams produced by three types of transducers: commercial PZT, air-backed PZT, and PZT ceramic/polymer composite. The signals were digitized and stored in two- and three-dimensional formats. The ANALYZE software package was used to produce movies of the traveling wave as well as the two- and three-dimensional depictions of the pulse at various points in space and time.

I. Introduction

Pulsed Acoustic Wave (PAW) is widely used in the fields of medical diagnosis [1], underwater acoustics [2], and nondestructive evaluation [3], etc. Usually the PAW in these fields is used for pulse-echo imaging in which high axial and lateral resolutions are required. The key element in pulse-echo imaging is acoustic transducers whose characteristics play an important role in high-resolution imaging. To evaluate and improve the performance of the transducer in pulse-echo imaging, it is helpful to study the spatial traveling characteristics of the PAW generated by the transducers.

This paper will discuss in detail the measurement and the movie display of pulsed acoustic waves in two- and three-dimensional formats for three types of transducers: commercial PZT, air-backed PZT, and PZT ceramic/polymer composite.

In section II, the measurement of PAW will be presented, and in section III, the two- and three-dimensional depictions of the PAW will be given. Finally, in section IV, we have a brief discussion.

*This work was partially supported under NIH CA 43920.

II. Measurement of PAW

Figure 1 is the block diagram of the experimental system. The probing transducer was fixed in the space, and a 0.5 mm diameter NTR System hydrophone (Model NP-1000) was used to measure the field. The hydrophone was scanned in two perpendicular directions by Superior Electric Synchronous/Stepping motors (Type M061-FD08E) in raster format. The motors were controlled by the computer in which the driving parameters of the motors were stored. A Polynomial Waveform Synthesizer (Model Data 2020) was used to generate unipolar sharp electrical excitation pulses and an 8-bit A/D converter was used to digitize the signal received by the hydrophone. The A/D converter was also controlled by computer and was synchronized to the motor motion as well as the wave emission. After the data were collected, they were displayed on a video monitor and stored on one inch tape. Then the stored data were transferred to a SUN workstation for multidimensional image processing.

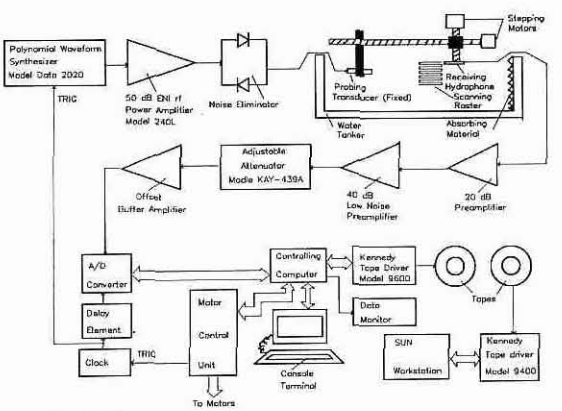

Fig. 1 Block diagram of the experimental system.

We assume that the transducers studied are circularly symmetric and the three-dimensional field representations of the PAW can be constructed by rotating the two-dimensional field around the axial axis of the transducers. Furthermore, we measured the field in the window aa'bb' (see Fig. 2) which was moved along with the PAW and was big enough so that the pressure field of the PAW outside this window was negligible as compared to the peak pressure of the PAW in the whole range of delay time concerned.

0090-5607/89/0000-0673 $1.00 © 1989 IEEE

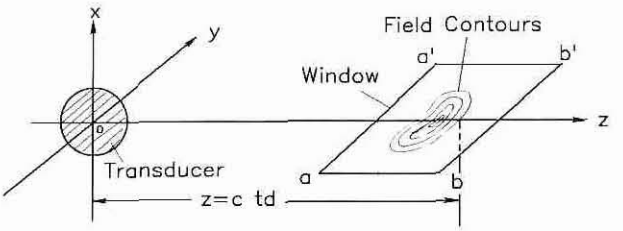

Fig. 2 Measurement window moving along with the PAW.

The fields were measured by changing the delay time to match the time interval between the emission of the acoustic wave and the beginning of the data acquisition. For each fixed delay time, the PAW had a unique spatial field distribution. The hydrophone was scanned in a raster format (see Fig. 1) to map the fields in planes through the axial symmetric axes of the transducers. The transducers were excited each time the hydrophone was moved to a new sampling position and the delay time was kept the same in each measurement. The backlashes of the driving screws were removed by dropping the even lines of data on the scanning raster.

Changing the delay time and repeating the procedure for the field measurement at a different spatial position results in a series of fields representing the wavefront of the PAW at different positions in space. Using the software ANALYZE [4], the three-dimensional fields were constructed and two- and three-dimensional measured pressure or intensity fields were displayed vividly as a movie.

III. Display of the PAW

Figure 3 shows ten successive windows corresponding to ten different spatial positions of the wavefront of the PAW in space at ten indicated delay times td_1 to td_{10}. Each of the windows is 20 mm (axial direction) x 96 mm (lateral direction) and connects to others in the axial direction without overlapping.

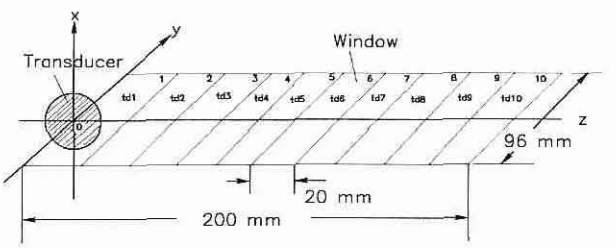

Fig. 3 Ten successive windows corresponding to ten delay times $td_1 \sim td_{10}$.

Figures 4, 5, and 6 are the images of the successive pressure fields of the PAW in the ten different windows shown in Fig. 3 for the commercial PZT, air-backed PZT, and the PZT ceramics/polymer transducers, respectively. The transducers were all unfocused and measured in water at room temperature. Their center frequency was about 2 MHz and diameters were 12.7 mm, 17.0 mm, and 17.0 mm, respectively. Each of the images was composed of 200 lines (lateral direction) and 400 columns (axial direction) and was of the size of the window in Fig. 3. The pixel size of these images was 0.48 mm (lateral) x 0.05 mm (axial). The labels 1 to 10 in these images indicated that the delay time was increased successively.

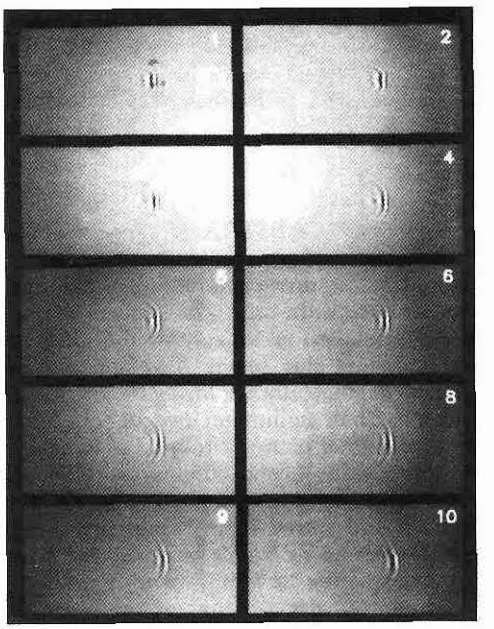

Fig. 4 Ten images of the PAW generated by the commercial PZT transducer with a sharp unipolar electrical excitation at ten successive delay times.

Figures 7, 8, and 9 are three-dimensional representations of the PAW corresponding to Figures 4, 5, and 6, respectively. They were obtained by first calculating the analytic signal and finding the envelopes of these images, then low-pass filtering the envelope images to get rid of some high-frequency noises and rotating them around the symmetric axis of the transducers. By choosing proper thresholds, binary images were obtained from which surfaces were detected and displayed with the ANALYZE software package. The thresholds for Figs. 7, 8, and 9 were 5, 5, and 7, respectively (the gray scale of these images was ranged from 0-255), and the surface images displayed were rotated clockwise 20° around the vertical axis. In these images, the rear and the side of the wave blobs can be seen clearly and the successive changes of the shapes of the wave blobs as a function of the delay time (or position) reveal the propagation characteristics of the PAW.

IV. Conclusion

An experimental system was set up for measurement of pulsed acoustic waves. Successive images of the two- and three-dimensional pressure fields of the pulses at different positions in space were constructed for three types of transducers.

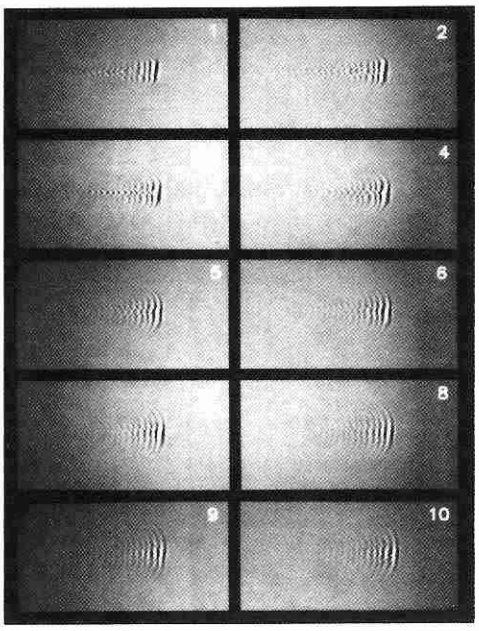

Fig. 5 Ten images of the PAW generated by the air-backed PZT transducer with a sharp unipolar electrical excitation at ten successive delay times.

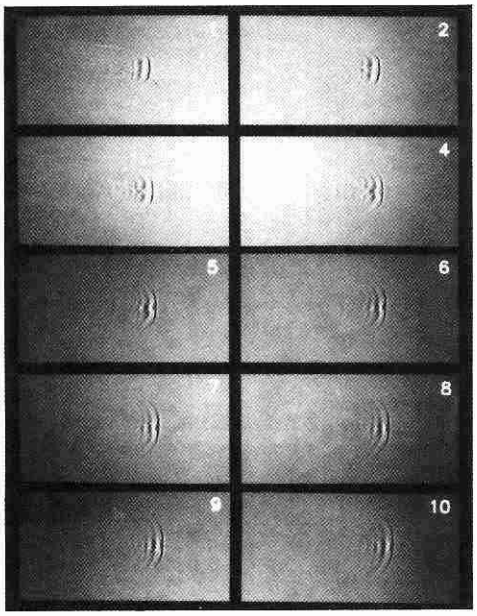

Fig. 6 Ten images of the PAW generated by the PZT ceramic/polymer composite transducer with a sharp unipolar electrical excitation at ten successive delay times.

The measurement method developed in this paper is also feasible for focused, linear, and unsymmetric transducers, etc.

From Figs. 4 through 9, one can deduce the field characteristics for each type of transducer. Therefore, images of two- and three-dimensional fields of transducers can be used to evaluate the performances of transducers in pulse-echo imaging. These new images give an unrivaled insight into the pulsed acoustic wave.

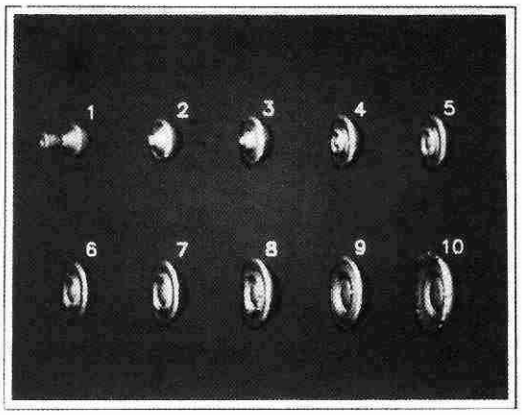

Fig. 7 Three-dimensional display of wave blobs of PAW at ten successive delay times for the commercial PZT transducer. The axial dimension of the pixels is about ten times smaller than the lateral dimensions.

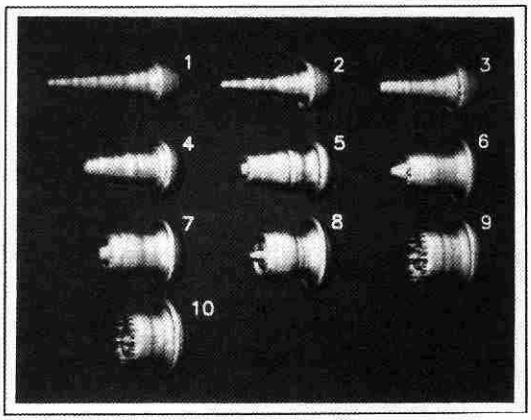

Fig. 8 Three-dimensional display of wave blobs of PAW at ten successive delay times for air-backed PZT transducer. The axial dimension of the pixels is about ten times smaller than the lateral dimension.

In addition, general information of the PAW can be obtained from Figs. 4 through 9: 1) pulsed waves exhibit low near and far field side lobes in the lateral direction which is quite different from the related behavior of the continuous wave, 2) the wavefront of the wave remains smooth both in the near and far field, 3) the ring-down oscillations of the narrow band transducers cause strong spatial interference that becomes smeared as the wave travels away from the source.

V. Acknowledgments

The authors wish to thank Elaine C. Quarve and Christine A. Welch for secretarial and graphics assistance, Mr.

William B. Harrison at Honeywell Ceramics Center for transducer design, and James A. Nicholson and Randall R. Kinnick for their development of the scanning system.

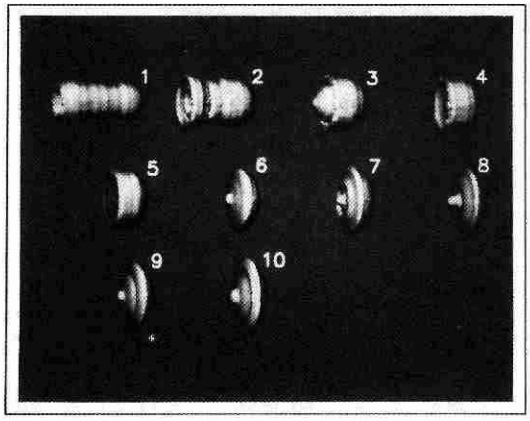

Fig. 9 Three-dimensional display of wave blobs of PAW at ten successive delay times for PZT ceramic/polymer transducer. The axial dimension of the pixels is about ten times smaller than the lateral dimension.

VI. References

[1] Kossoff, G.: Progress in pulse-echo techniques. Ultrasonics in Medicine, Exerpta Medica 309:37-42, 1974.

[2] Chakraborty, B.: Effects of scattering due to seafloor micro relief on a multifrequency sonar seabed profiler. Journal of the Acoustical Society of America 85(4):1478-1481, April, 1989.

[3] Kino, G.: Acoustical imaging for nondestructive evaluation. Proceedings of the IEEE 67(4):510-525, April, 1979.

[4] Robb, R. A. and C. Barillot: Interactive display and analysis of 3-D medical images. IEEE Transactions on Medical Imaging 8(3):217-226, September, 1989.